J Nanostruct 14(3): 905-916, Summer 2024

RESEARCH PAPER

Electrochemical and in Vitro Bioactivity of Niobium Nitride Coatings on Ti6Al4V Alloy Bio-Implants

Qutaiba Khalaf Mahmood [1]*, Chiheb Chaker [2], Mohammed K. Khalaf [3], Hanen Chaker [4]

[1] *North Refineries Company, Ministry of Oil, Iraq*

[2] *Laboratory of Multifunctional Materials and Applications (LaMMA), LR16ES18, University of Sfax, Faculty of Sciences, Sfax, Tunisia*

[3] *Ministry of Higher Education and Scientific Research, Baghdad, Iraq*

[4] *Laboratory of Materials and Environment for Sustainable Development (LR18ES10), University of Tunis El Manar, ISSBAT, Tunis, Tunisia*

ARTICLE INFO

Article History:
Received 03 May 2024
Accepted 26 June 2024
Published 01 July 2024

Keywords:
Corrosion biomedical applications
Niobium nitride films
Radio frequency sputtering
Ti6Al4V Alloy

ABSTRACT

Niobium Nitride (NbN) film deposition has emerged as a pivotal process in modifying the surface properties of the Ti6Al4V alloy, a material widely recognized for its excellent mechanical properties and biocompatibility. This innovative approach not only enhances the alloy's suitability for various medical applications but also paves the way for future advancements in biomedical technology. By applying NbN films to the surface of Ti6Al4V, researchers are addressing critical challenges in medical device performance, particularly in the areas of wear resistance and corrosion resistance, which are essential for the longevity and reliability of implants. The microstructural morphologies of the thin films were assessed through field emission scanning electron microscopy, highlighting the significant impact of NbN nanoparticles on the surface characteristics of the nanocoated Ti6Al4V. Electrochemical studies conducted through cyclic polarization measurements indicated a decreased corrosion rate of 4.02 $\times 10^{-4}$ mmpy for the sputter-deposited samples compared to 4.79 $\times 10^{-1}$ mmpy for the uncoated sample. In vitro biocompatibility characterization in simulated body fluid demonstrated the growth of a hydroxyapatite layer on the NbN-coated Ti6Al4V surface, with its relative thickness increasing at higher sputtering power and substrate deposition temperature. These findings underscore the superior biocompatibility and enhanced corrosion protection of nanostructured NbN coatings over Ti6Al4V compared to uncoated Ti6Al4V specimens.

How to cite this article
Mahmood Q., Chaker C., Khalaf M., Chaker H. Electrochemical and in Vitro Bioactivity of Niobium Nitride Coatings on Ti6Al4V Alloy Bio-Implants. J Nanostruct, 2024; 14(3):905-916. DOI: 10.22052/JNS.2024.03.019

INTRODUCTION

Due to their low modulus of elasticity, corrosion resistance, and biocompatibility, titanium and its alloys are often considered the best choice among metallic implant materials for bone implant applications [1]. Unfortunately, the extensively used Ti6Al4V alloy lacks adequate wear resistance, accelerating electrochemical interactions between the implant surface and the physiological environment due to wear-induced debris [2]. Furthermore, the discharge of V and Al ions into human tissue compromises the alloy's

* *Corresponding Author Email: mohammedkhkh@yahoo.com*

biocompatibility, as Al can cause neurological illnesses and V ions can harm cells [3]. Hence, it is essential to pursue further advancements that enhance these implant materials' durability and biological effectiveness. *Total joint replacement* (TJR) arthroplasty is a surgical procedure in which artificial biomaterials are used to replace natural joints. This is done when the body's biological repair processes fail or when excessive loading conditions lead to early joint degradation. [4-6]. The two primary areas of study in biomaterials are the development of new metallic materials with mechanical properties similar to human bone, and the improvement of surface modification techniques that enable optimal biocompatibility and osseointegration of medical alloy implants [7-8]. Nanoparticles, due to their nanoscale dimensions, can be incorporated into surface modification techniques to create coatings with enhanced bioactivity and improved biological responses. Similar to their use in drug and vaccine delivery systems [9] due to their ability to target specific cells and enhance immune responses and in gene therapy [10], where they facilitate targeted cellular interactions, nanoparticles can improve the osseointegration of titanium alloys by promoting better cellular adhesion and minimizing inflammatory responses. Additionally, artificial intelligence (AI) driven models can accelerate the discovery of new nanoparticle-based coatings by predicting material properties and identifying ideal configurations for specific biomedical applications [11]. Alloys used as orthopedic biomaterials have high specific strength and corrosion resistance. These alloys develop a natural passivation oxide layer on their surface that protects them from accelerated corrosion rate and functions as an electrical resistor to delay the anodic dissolution of metal cations. As a result, the rate of uniform, gradual, finite corrosion in vivo for all implant alloys is known.

However, greater surface damages to this passivation layer, such as that caused by fretting or wear, may create circumstances that encourage rapid focused corrosion and failure. Metal alloys, including titanium alloys like commercially pure titanium (cpTi), Ti-6Al-4V, stainless steels, Co-Cr-Mo alloys, etc., are widely used to make implant materials. Titanium alloys have been used for surgical implants since the 1940s, and commercially pure titanium (cpTi) is used in implants due to its superior corrosion resistance and great tissue compatibility. However, its application can be hindered by low strength and wear resistance. The Ti-6Al-4V alloy used in prostheses grew in the late 1970s due to its superior corrosion resistance, caused by an oxide coating that spontaneously forms on the surface when exposed to air (passivation ability), and outstanding mechanical qualities. Ti6Al4V became the best Titanium alloy and is now widely used in automotive, aerospace, chemical, marine, and biomedical industries. About 50% of the world's total Titanium production is covered by the Ti6Al4V alloy [12-15]. According to biocompatibility studies, Al and V in the Ti6Al4V alloy can cause corrosion and release ions that may enter the human body, leading to oxygen depletion and high concentrations of the elements in surrounding tissues. Vanadium can cause cytotoxic effects, while aluminum can soften bones and damage neurons. However, surface modification techniques have been employed to limit ion exchange in the body environment, thus improving the alloy's surface characteristics, corrosion resistance, and passivation capacity [16, 17].

NbN, a transition metal nitride, has become popular recently due to its high hardness, melting temperature, and wear resistance [18, 19]. It is widely used as an emission cathode and in coating materials to enhance their resistance to chemical corrosion [20]. NbN is suitable for various applications in microelectronics, sensors, optical films, micromechanics, and coating wear resistance or chemical corrosion due to its chemical inertness and temperature stability. Various techniques have been employed to create NbN thin films, including reactive magnetron sputtering, ion beam-aided deposition, pulsed laser deposition, and filtered arc deposition [21]. To assess biocompatibility, a coated sample was immersed in Simulated Body Fluid (SBF) for a month, which can generate biomimetic apatite on bioactive surfaces [22]. One promising material to enhance Ti alloys' biocompatibility is nanostructured NbN coatings, which have superior mechanical strength, corrosion resistance, and bio-inertness [12]. Although its use in orthopedics and dentistry has been limited due to its high cost and extreme hardness, covering Ti alloy substrates with a layer of NbN film can offer a favorable compromise between corrosion and wear resistance [13].

This study focuses on fabricating NbN coatings over biomedical Ti6Al4V alloy by employing a

Radio Frequency (RF) sputtering method for orthopedic implant applications. The aim is to investigate the applicability of NbN coating on Ti6Al4V alloy to enhance bioactivity and corrosion protection performance in SBF.

MATERIALS AND METHODS

The deposition of NbN coatings was carried out on Ti6Al4V alloy substrates with a diameter of 2 cm. Ti6Al4V alloy samples were prepared and smoothed using silicon carbide polishing paper with a particle size of 500 microns. Subsequently, they were chemically cleaned with HF: HNO_3:H_2O = 4:10:86. The samples were washed with 96% ethanol using an ultrasound bath for 10 minutes and repeated twice. The samples were washed with distilled water using an ultrasound bath for 10 minutes. NbN thin films were deposited onto Ti6Al4V alloy substrates via RF reactive magnetron sputtering using an Nb (99.95%) target (50 mm diameter and 3 mm thick) in a commercial high-volume, fully automated coating tool (CRC-600 system, Torr Inc., USA) in the presence of a mixture of argon and nitrogen (20 %) with flow rate 20 *SCCM*. Typically, this low-pressure RF sputtering system operates at 13.56 MHz and power of up to 300 watts.

Before deposition, the system was evacuated to a base pressure of 1.0 x 10^{-5} torr. The system was then backfilled to a pressure of 1.0 x 10^{-2} torr for target plasma cleaning and sputter etching of the Ti6Al4V alloy substrate in an Ar: N_2 atmosphere. The distance between the cathode and the anode electrode of the magnetron is 10 cm. The RF sputtering power gradually varied from 80 to 160 watts, while the depositing substrate temperature varied from 40 to 200 °C. The Field Emission Scanning Electron Microscopy (FESEM) images carried out by (FESEM, Inspect TM F50, FFI Company, Neverland), and the total range of magnification was 10 kX to 100kX. Microhardness measurements were performed on uncoated and NbN coated Ti6Al4Vspecimens surface with a made Vickers Microhardness tester (HV-100, Japan) using 0.24N load for the 20s and three readings were taken to determine the average value. Corrosion tests were conducted using a PARSTAT 2273 from the USA, employing SBF as the corrosion environment. Potentiodynamic cyclic polarization of both coated and uncoated samples was performed in a prepared SBF solution with a chemical composition detailed in Table 1, adjusted to pH 7.4. The potential was applied to the working electrode at a scan rate of 0.167 mVs^{-1} from the open circuit potential. Corrosion rates were determined through Tafel plot analysis, and the results were expressed in mmpy.

All measurements were conducted at least three times, demonstrating good reproducibility. Biocompatibility assessments included optical microscope imaging and XRD patterns for the surfaces of coated and uncoated Ti6Al4V alloy samples immersed in a SBF solution for three weeks. The optical microscope used the type of Nikon 1200F- Japanese company Nikon camera image to observe the Hydroxyapatite (HAp) layer formed after immersing in SBF solution for two weeks. The structural properties of the formed HAp layer and NbN films were obtained by the X-ray diffraction type of Shimadza XRD -6000 using CuK_α and λ = 0.15406 nm radiation.

RESULT AND DISCUSSION

Field Emission Scanning Electron Microscopy

The experiments described in the text were conducted using NbN films deposited onto Ti6Al4V substrates, except for the FESEM images, which were taken using glass substrates. The FESEM images of NbN films deposited on glass substrates at different sputtering power and substrate temperatures are presented in Figs. 1 and 2. These images show the presence of nanoparticles and non-uniform clumps, which led to the formation of clusters (Fig. 1a). Furthermore,

Table 1. Chemical composition of Simulated Body Fluids (SBF).

Item	Description	Quantity g/l
1	NaCl	8.036
2	KCl	0.223
3	$CaCl_2$	0.293
4	$NaHCO_3$	0.352
5	K_2HPO_4	0.230
6	$MgCl_2.6H_2O$	0.311
7	$NaSO_4$	0.072

the surfaces of the thin films were uniformly and homogeneously covered with particles, with particle size increasing with an increase in sputtering power and deposition rate (Fig. 1b, c). The average particle size of the deposited NbN films ranged from 17-33 nm. This is in line with previous studies [23-25], which found that higher deposition powers result in films with a lower inclusion of impurities and fewer voids due to the higher energy of the sputtering gas. The surface morphology of all deposited coatings using higher sputtering powers and substrate temperatures

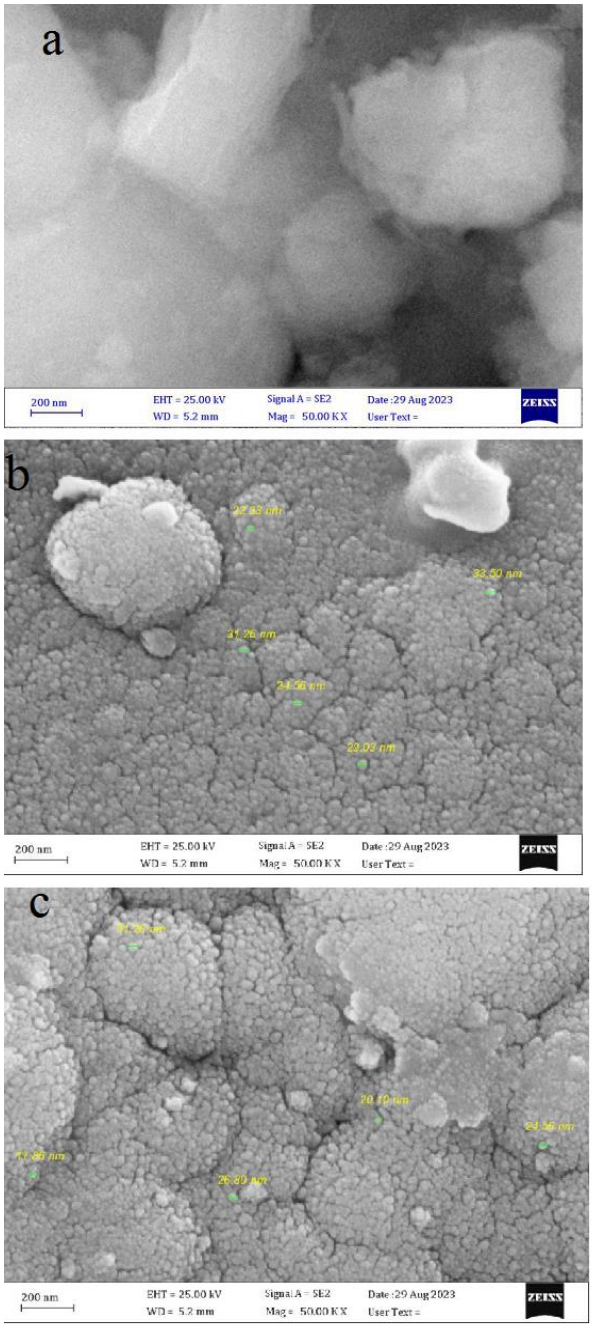

Fig. 1. FESEM images for nanoparticles of NbN thin film coating deposited on Ti6Al4V substrates at sputtering power of (a) 80 W, (b) 120 W, (c) 160 W and depositing substrate temperature of 40 °C.

unequivocally demonstrated an increase in film thickness, resulting in significantly larger grain size, roughness, and markedly improved adhesion of the coatings. It is an indisputable fact that high sputtering power leads to a substantial increase in the deposition rate due to the superior energy of argon compared to the target species, unequivocally leading to the ejection of atoms

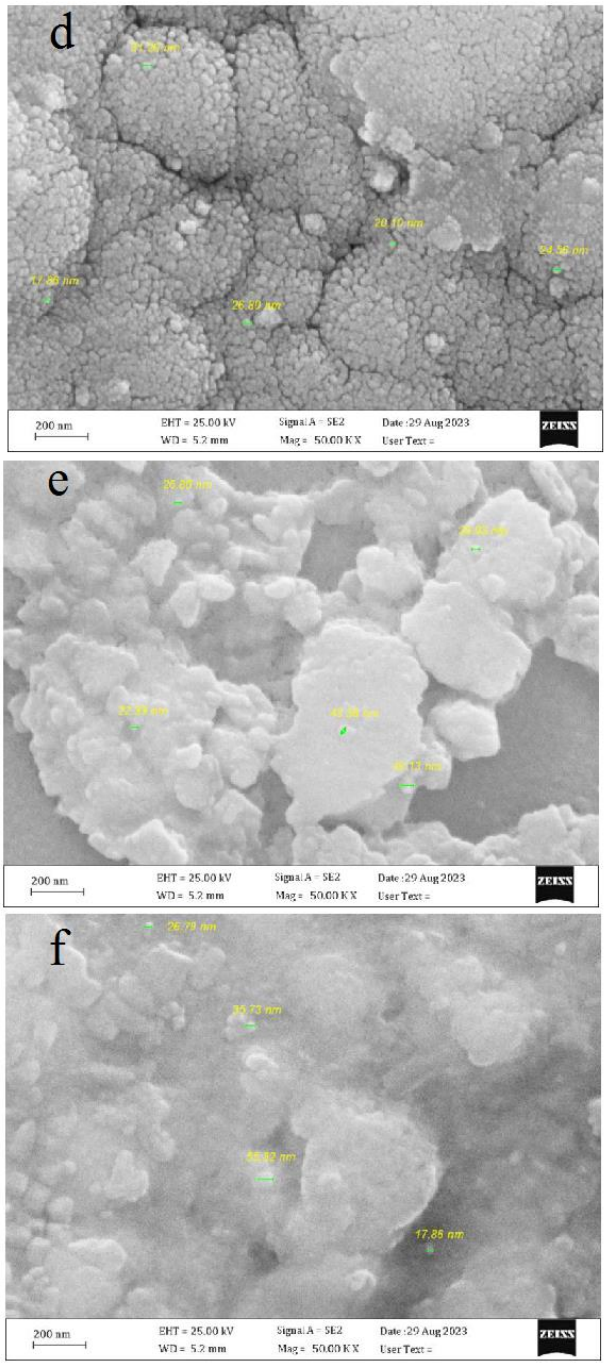

Fig. 2. FESEM images for nanoparticles of NbN thin film coating deposited on Ti6Al4V substrates at sputtering power of 160 W and depositing substrate temperature of (d) 40 °C, (e) 125 °C and (f) 200 °C.

from the target material. This undeniable increase in thin film thickness is unambiguously attributed to the higher concentration of charged particles. The increased energy of these particles enhances the reactive processes, contributing to the formation of a thicker layer [26].

It has been observed that the particle size of NbN increases when sputtered NbN films are deposited at substrate temperatures of 125 °C and 200 °C. The average particle size of NbN thin films increases from 17 nm to 55 nm, respectively. The increase in substrate temperature leads to an increase in the crystalline of the film, which provides additional energy to the datoms, resulting in an improvement in the order of the microstructure and particle size. However, excessive sputtering power and substrate temperature may lead to a degradation of the preferred orientation and the film may experience the impact of highly energized particles. Additionally, the difference in the thermal expansion coefficients between the glass substrate and NbN coating can lead to the formation of internal defects in the film. These defects can ultimately compromise the quality of the film, as mentioned in reference [27].

Electrochemical corrosion measurements

This study delves into the corrosion resistance of NbN coatings in a SBF solution, using potentiodynamic and potentiostatic polarization tests. Fig. 3 shows the active behavior observed in potentiodynamic polarization curves for all specimens, and Tafel extrapolation provided electrochemical features, which we've summarized in Table 2. The findings show a significant reduction in corrosion rate from 4.79×10^{-1} mmpy to 4.02×10^{-4} mmpy for uncoated Ti6Al4V alloy and NbN-coated samples, respectively. Notably, the coated samples exhibited a shift in corrosion potential towards the cathode side, and a wider passivation region, as indicated in Fig. 3. The results for Ti6Al4V samples coated at different sputtering power and

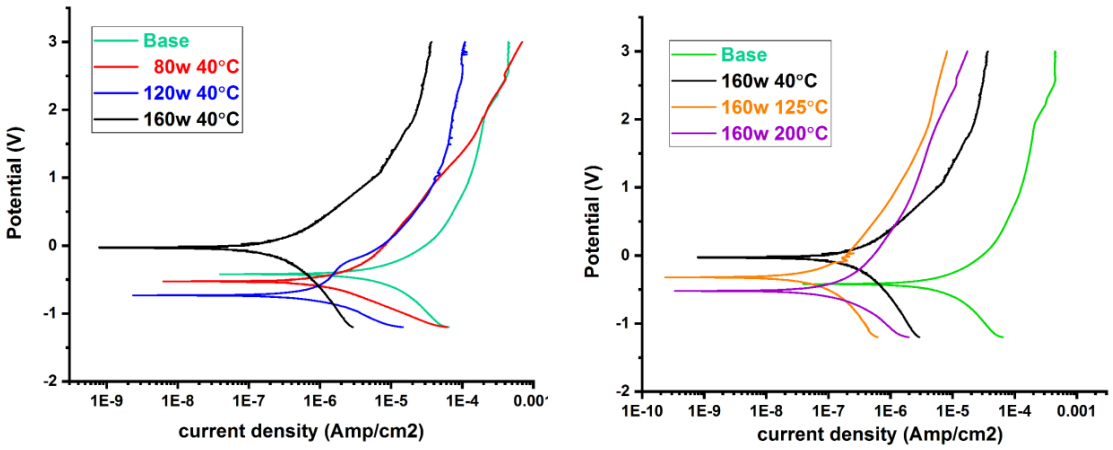

Fig. 3. Polarization curves Tafel for uncoated Ti6Al4V alloy (base), and coated by NbN films deposited with different sputtering power and depositing substrate temperature.

Table 2. Corrosion measurements for uncoated and NbN coated Ti6Al4V alloy substrates deposited with different sputtering power and depositing substrate temperature.

ITEM	E corr. (Volt)	I corr. (Amp.)	Corr. Rate (mmpy)	Corr. Rate (mdd)	βc	βa	OCP (Volt)
base	-0.426	2.542×10^{-6}	2.212×10^{-2}	4.787×10^{-1}	0.214	0.200	-0.483
Q9	-0.533	7.517×10^{-7}	6.229×10^{-3}	1.348×10^{-2}	0.196	0.195	-0.447
Q10	-0.725	5.051×10^{-7}	4.396×10^{-3}	9.154×10^{-3}	0.177	0.252	-0.436
Q11	-0.021	1.242×10^{-7}	1.080×10^{-3}	2.337×10^{-3}	0.229	0.200	-0.421
Q12	-0.314	2.136×10^{-8}	1.859×10^{-4}	4.023×10^{-4}	0.199	0.204	-0.194
Q13	-0.509	5.164×10^{-8}	4.494×10^{-4}	9.726×10^{-4}	0.182	0.211	-0.326

the same depositing temperature, however, are even more remarkable. The polarization curves have an irregular effect where it has a cathodic effect for the Q9 and Q10 samples, changing to an anodic effect for the Q11 sample. This is because the coated sample has a mixed effect due to a decrease in NbN coating thickness, which is related to de-sputtering at the power of 120W

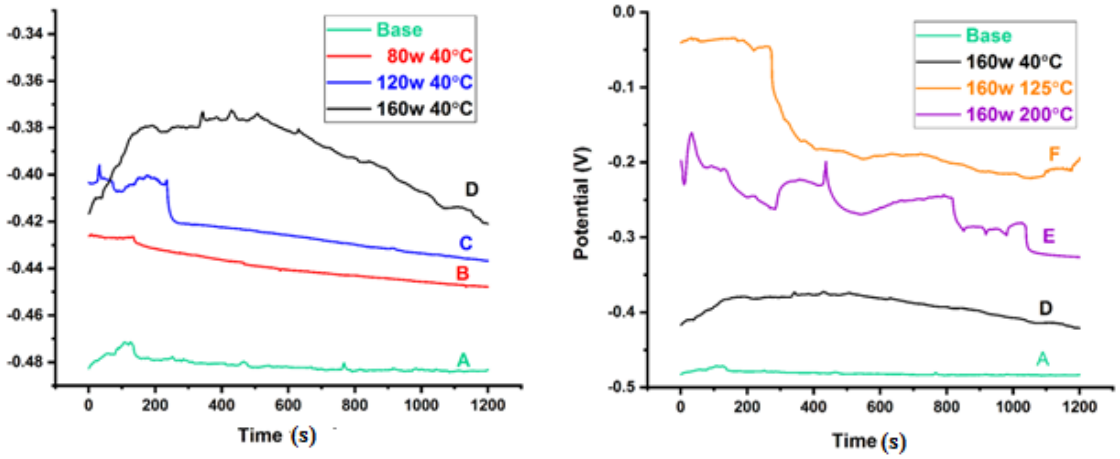

Fig. 4. Open-circuit potential variation with time curve of uncoated and NbN coated Ti6Al4V alloy substrates deposited with different sputtering power and depositing substrate temperature.

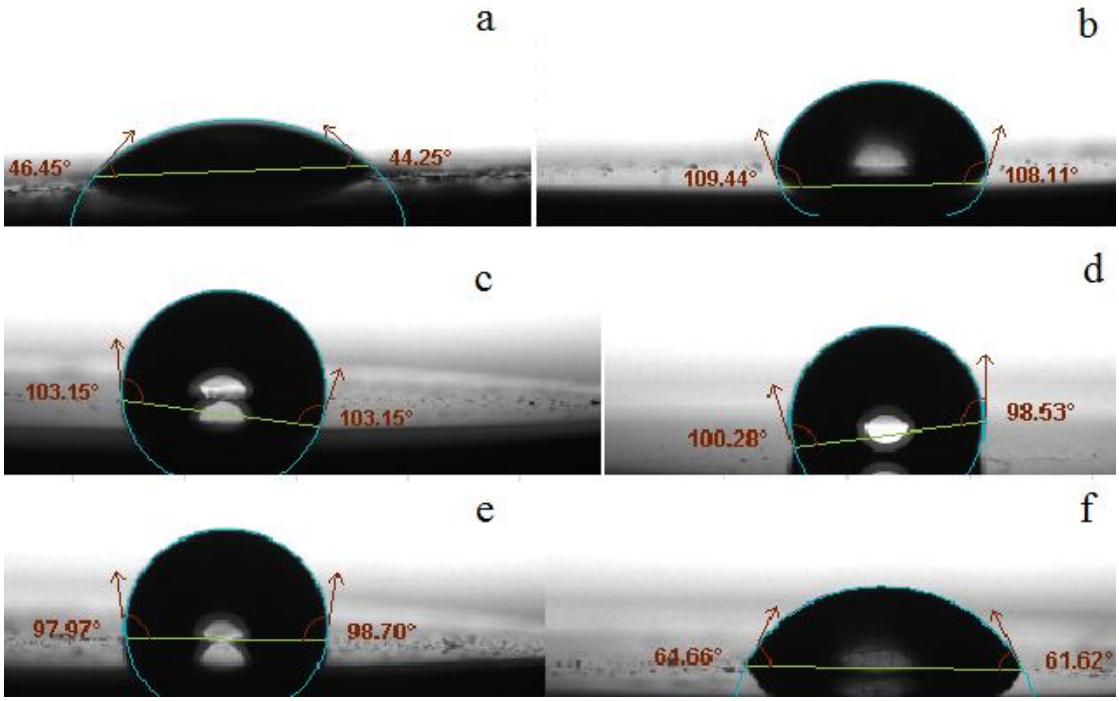

Fig. 5. The contact angle measurements for water droplets on uncoated (a) and NbN coated Ti6Al4V samples with (b) 80W, (c) 120W, (d) 160W at depositing substrate temperature of 40 °C and sputtering power of 160W at depositing substrate temperature of (e) 125 °C, (f) 200 °C.

and depositing temperature of 40 °C. However, for Ti6Al4V samples coated at the same sputtering power and different depositing temperatures, the cathodic polarization always reduces the corrosion rate as shown in Fig. 3.

Fig. 4 shows the open-circuit potential (OCP) variation with immersion time in the SBF solution at 30 °C for uncoated Ti6Al4V alloy and NbN-coated films. The initial OCP for uncoated Ti6Al4V was -0.483V, gradually increasing to -0.194V for NbN-coated samples. Overall, the coated samples exhibited a positive shift in corrosion potential, reduced corrosion current, and lower corrosion rate values compared to the base substrate, proving that NbN coatings have good corrosion resistance properties.

These results suggest the formation of a passive layer, with the superior corrosion behavior of Nb-based coatings attributed to their higher nobility and greater thermodynamic stability, as supported by previous studies [18-21]. The enhanced corrosion resistance of coatings deposited at higher temperatures is linked to their homogeneous and compact morphology, coupled with superior hydrophobic properties that facilitate water removal, thereby improving

Table 3. The contact angle measurements on the uncoated and NbN coated Ti6Al4V alloy substrates deposited with different sputtering power and depositing substrate temperature.

Samples	Sputtering power (watt)	Substrate temperature (°C)	Contact angle (degree)		Type of Hydrophoilic
			Right	Left	
Q1 (Ti6Al4V uncoated)			46.45	44.25	
Q9 NbN	80	40	109.44	108.11	phobic
Q10 NbN	120	40	97.97	98.11	phobic
Q11 NbN	160	40	103.15	103.15	phobic
Q12 NbN	160	120	100.28	98.53	phobic
Q13 NbN	160	200	64.66	61.62	phlic

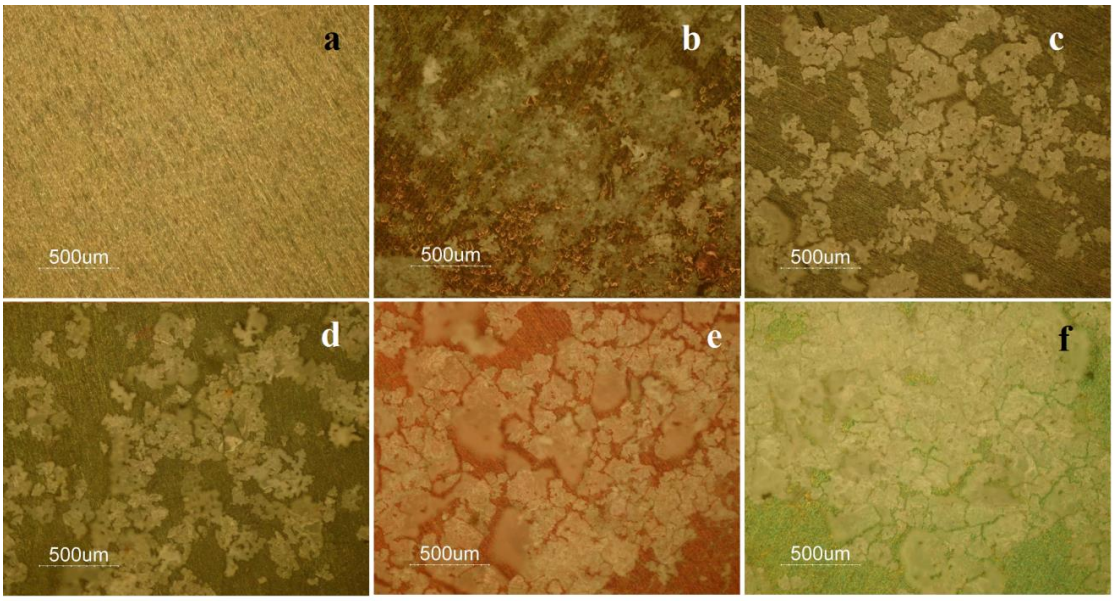

Fig. 6. The optical microscopy, of (a) uncoated base of Ti6Al4V alloy, and the NbN coated Ti6Al4V alloy samples structures with different sputtering power (b) 80 W, (c) 120 W, (d) 160 W at 40 °C, and different depositing temperatures (e) 160 W at 125 °C, (f) 160 W at 200 °C.

anti-corrosion behavior [15].

Contact Angle (CA) and Wettability

Wettability is assessed through contact angle measurements, with lower angles indicating greater wettability (≤ 90°) and higher angles indicating lower wettability (≥ 90°). In the context of biocompatible materials, wettability plays a crucial role in bone apposition, cell adhesion, and implant stability [28]. A contact angle refers to the angle made between a solid/liquid/gas interface on a surface, specifically the angle between a plane tangent to a liquid droplet and a plane containing the surface where the liquid is deposited. Fig. 5 and Table 3 present contact angle measurements for water droplets on uncoated and coated Ti6Al4V samples. The variations in contact angle for coated Ti6Al4V samples at different sputtering power and substrate temperatures are depicted. Material wettability and surface energy are significant factors influencing cell adhesion and proliferation on implant materials. The contact angles of NbN films on Ti6Al4V alloy surfaces are notably higher than those of the bare Ti6Al4V alloy substrate, indicating lower wettability (hydrophobic surface).

The positive effect of NbN coatings on Ti6Al4V alloy is evident as the contact angle increases, transforming the surface from hydrophilic to hydrophobic. The randomness in angle values is attributed to differences in thickness, density, and the formation of a layer on the NbN thin film surface. The increase in coating thickness, associated with higher depositing substrate temperatures, results in increased roughness parameters. This linear trend in roughness reflects the sputtering process's ability to produce a rough characteristic, providing a larger surface area. The variation in the observed angles for the same drop may be due to the drop's evaporation over time. In such cases, we attempted to minimize air flow

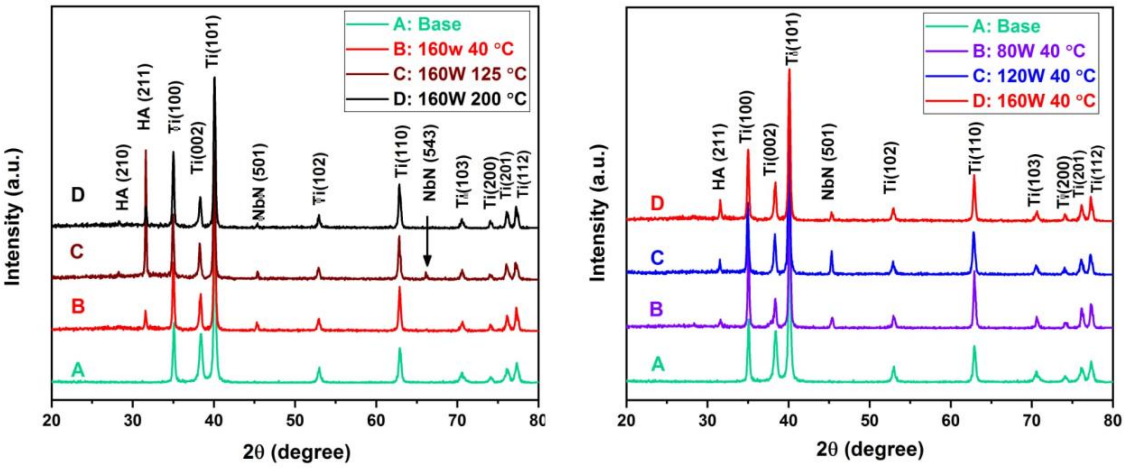

Fig. 7. The XRD of uncoated and NbN coated Ti6Al4V alloy substrates deposited with different sputtering power and depositing substrate temperature.

Table 4. Ion release for uncoated and NbN coated Ti6Al4V alloy substrates (160Watts, 200 °C) for testing in SBF solution after one month of immersion.

Element	Uncoated (Ti6Al4V) ppb	NbN/Ti6Al4V sample 1 ppb	NbN/Ti6Al4V sample 2 ppb	NbN/Ti6Al4V sample 3 ppb	NbN/Ti6Al4V Average ppb
Nb	0.0	178.0	112.0	140	143.3
Al	62.0	48	50	55	51
Ti	84	75	73	68	72
V	5.3	3.0	1.8	2.6	2.4

over the sample as much as possible and waited long enough for the drop to stabilize. The average of the left and right contact angles can then be reported as the result.

The alteration in the contact angle value of Q13 NbN is attributed to the reduction in the thickness of the NbN coating and the concurrent decrease in the roughness of the coated sample surface. This transformation is a result of re-sputtering at a working power of 160 watts and a depositing substrate temperature of 200 °C, leading to a shift toward a more hydrophilic nature. Sputter-coated Ti6Al4V exhibits enhanced hydrophobic and a larger surface area due to its rougher profile compared to uncoated Ti6Al4V. Consequently, the Ti6Al4V surface transitions to hydrophobic after an increase in depositing substrate temperature during the coating process. A more hydrophobic material tends to reduce the corrosion rate as its interaction with the liquid or environment diminishes [28]. This characteristic is beneficial for antibacterial efficacy, as a hydrophobic surface can alter the environmental surface, reduce microbial adherence, and ultimately decrease the incidence of infections [29].

Biocompatibility

Biocompatibility tests were done in SBF for uncoated Ti6Al4V alloys and coated with NbN films with different sputtering power and different depositing temperatures. The optical microscopy and XRD properties of the base of Ti6Al4V alloy, and the NbN/Ti6Al4V samples were evaluated because they can be linked with alloy biocompatibility [30, 31]. The biocompatibility test for the NbN-coated Ti6Al4V alloy samples took three weeks, and the camera images of an optical microscope were taken for both the uncoated substrate and the coated samples as shown in Fig. 6.

The photographs of the samples after being immersed in SBF solution clearly show the formation of a dense and uniform bone-like apatite (HAp) layer on the surfaces of the samples. In Fig. 6, optical microscope photographs of precipitated HAp coatings are displayed. The HAp particles appear as bright spots on the darker area of the Ti6Al4V substrate. The figures demonstrate that increasing sputtering power leads to greater surface coverage and thickness of the HAp coating. Additionally, the substrate temperature during deposition affects the amount of deposited HAp particles on the Ti6Al4V substrate's surface. The high temperature of the deposition substrates leads to increased deposition of the NbN nanoparticle layer increasing the density of the deposited HAp particles when immersed in the SBF solution [26, 32-36]. This HAp layer was formed from the SBF, which ensured the biocompatibility of the coating layer. The optical microscope test revealed the appearance of agglomerated HAp on the samples after being immersed in the SBF solution. For the microscopy test images of all samples, the high agglomeration of HAp was visible on the sample coated with NbN thin films. The XRD pattern illustrated in Fig. 5 showed two new peaks on the positions at 28.96° and 31.77°, corresponding to the orientation (210) and (211) matching the standard XRD standard card ICDD 09-0432, indicating the deposition of the Calcium Phosphate crystal layer [32]. The peaks characteristic for crystal planes of HAp are indicated in Fig. 5. The presence of these peaks in all samples corresponds to the crystal plane of HAp, which is in strong agreement with the experimental results and analysis conducted by Strzała et al., (2012) [33]. The XRD analysis decisively confirms the formation of the HAp coating. The other peaks belong to the titanium element in the alloy [34-36]. This indicated that the HAp layer is formed after immersing in simulated body fluid for three weeks as shown in Fig. 5. This feature of HAp may be of great importance for implant fixation. This formed layer for SBF has ensured the biocompatibility of the Ti-coated layer [32].

Ion Release Evaluation

To reveal the ion release we choose the samples uncoated Ti6Al4V alloy and NbN/Ti6Al4V (160 Watts, 200 °C) for testing in 100 ml of SBF solution after one month of emersion in parts per billion. Four samples of NbN/Ti6Al4V (160 Watts, 200 °C) were used, and then taking average results. According to Table 2, it is evident that the corrosion rate of the NbN-coated Ti6Al4V sample is significantly lower than that of the uncoated sample. The corrosion rate without coating is 4.79×10^{-1} mmpy, whereas the NbN-coated Ti6Al4V sample exhibited a corrosion rate of 4.02×10^{-4} mmpy. This substantial difference can be attributed to the protective barrier provided by the NbN coating, which effectively hinders the release of metal ions from the Ti6Al4V. Additionally, the lower Icorr value for the coated

sample further confirms its superior corrosion resistance. These findings are consistent with the conclusions drawn by Dihn et al. [37], who elaborated on the higher Icorr value expected for uncoated Ti6Al4V compared to the coated sample. Table 4 summarizes the results of ion release. Ti, Al, and V ions for uncoated specimens and coated specimens are released during the corrosion process in the physiological environment. A decrease in their release can be observed for the coated surface-modified samples. Therefore, it can be assumed that the proposed inorganic treatment can reduce the release of metal ions, due to the higher thickness of the nitric layer formed, compared to the original layer, which improves biocompatibility. Also, ion release decreases, which can attributed to the improvement of the anti-corrosion properties and the barrier effect of the NbN coating that prohibits the ions release into the immersion solution [37, 38]. We note from the concentrations of the ions released, especially vanadium, that these concentrations are among the permissible quantities and do not constitute a defect in the biological use of this treated alloy. Our results; lowest ion release of vanaduim, high corrosion resistance, excellent biocompatibility, and cytocompatibility of NbN and Ti6Al4V are satisfy the criteria required by biomedical applications [39, 40].

CONCLUSION

NbN coatings were successfully applied to biomedical Ti6Al4V alloy through RF sputtering deposition. A comprehensive study was conducted to explore the impact of sputtering power and substrate temperature in RF magnetron sputtering on the growth characteristics of NbN thin films on both Ti6Al4V alloy and glass substrates. The deposition of NbN thin films was carried out at varied sputtering powers and substrate temperatures, with other experimental parameters such as working pressure, target-to-substrate distance, and deposition times held constant. The findings revealed a consistent grain-like morphology across all deposited coatings, with a comparable top surface appearance observed for NbN coatings deposited at elevated sputtering power and substrate temperatures. Field Emission Scanning Electron Microscopy images of the deposited samples at different sputtering powers and substrate temperatures illustrated the presence of nanostructures, with increased agglomeration as sputtering power and substrate temperature rose. Electrochemical assessments conducted on the coated samples displayed a noticeable improvement in corrosion resistance, as evidenced by a positive shift in corrosion potential, reduced corrosion current, and lower corrosion rate values when compared to the base substrate. This provides strong evidence for the excellent corrosion resistance properties of NbN coatings. This advancement in alloy properties holds significant promise for medical applications, particularly in surgical implants.

ACKNOWLEDGEMENTS

We offer all respect, appreciation, and gratitude to the Ministry of Higher Education and Scientific Research - Science and Technology, Baghdad, Iraq, and the Laboratory of Multifunctional Materials and Applications (LaMMA), Faculty of Sciences of Sfax, University of Sfax, Tunisia.

CONFLICT OF INTEREST

The authors declare that there is no conflict of interests regarding the publication of this manuscript.

REFERENCES

1. Nikolova M, Ormanova M, Nikolova V, Apostolova MD. Electrochemical, Tribological and Biocompatible Performance of Electron Beam Modified and Coated Ti6Al4V Alloy. Int J Mol Sci. 2021;22(12):6369.
2. Ching HA, Choudhury D, Nine MJ, Abu Osman NA. Effects of surface coating on reducing friction and wear of orthopaedic implants. Science and technology of advanced materials. 2014;15(1):014402-014402.
3. Balla VK, Bose S, Davies NM, Bandyopadhyay A. Tantalum—A bioactive metal for implants. JOM. 2010;62(7):61-64.
4. Zhou R, Wei D, Cao J, Feng W, Cheng S, Du Q, et al. Synergistic Effects of Surface Chemistry and Topologic Structure from Modified Microarc Oxidation Coatings on Ti Implants for Improving Osseointegration. ACS Applied Materials & Interfaces. 2015;7(16):8932-8941.
5. Zhang BGX, Myers DE, Wallace GG, Brandt M, Choong PFM. Bioactive coatings for orthopaedic implants-recent trends in development of implant coatings. Int J Mol Sci. 2014;15(7):11878-11921.
6. Long M, Rack HJ. Titanium alloys in total joint replacement—a materials science perspective. Biomaterials. 1998;19(18):1621-1639.
7. Richardson T, Esterhuizen TM, Engelbrecht AL, Slogrove AL. Recognition of infants at high risk for vertical HIV transmission at delivery in rural Western Cape Province, South Africa. S Afr Med J. 2022;112(11):860-865.
8. Khalid Naji Q, Mohammed Salman J, Mohammed Dawood N. Plasma Electrolytic Oxidation of Nanocomposite Coatings on Ti-6Al-7Nb alloy for Biomedical Applications. Baghdad Science Journal. 2024;21(11):3554-3569.
9. Al-Abboodi A, Mhouse Alsaady HA, Banoon SR, Al-Saady

M. Conjugation strategies on functionalized iron oxide nanoparticles as a malaria vaccine delivery system. Bionatura. 2021;3(3):2009-2016.
10. Rabeea Banoon S., Mahdi, D. S., Gasaem, N. A., Abed Hussein, Z., & Ghasemian, A.. The Role of Nanoparticles in Gene Therapy: A Review. Journal of Nanostructures, 14(1), 48-64(2024).
11. Hassan, S. A., Almaliki, M. N., Hussein, Z. A., Albehadili, H. M., Banoon, S. R., Al-Abboodi, A., & Al-Saady, M.. Development of Nanotechnology by Artificial Intelligence: A Comprehensive Review. Journal of Nanostructures, 13(4), 915-932(2023).
12. Basiaga M, Kajzer W, Walke W, Kajzer A, Kaczmarek M. Evaluation of physicochemical properties of surface modified Ti6Al4V and Ti6Al7Nb alloys used for orthopedic implants. Materials Science and Engineering: C. 2016;68:851-860.
13. Antonelli G. 1. Introduction. Springer Tracts in Advanced Robotics: Springer-Verlag. p. 1-13.
14. Wong JY, Bronzino JD. Biomaterials. CRC Press; 2007.
15. Khalaf MK. Effect of sputtering power on optical Properties of RF sputtering deposited Ti6Al4V Thin Films. Iraqi Journal of Physics. 2019;15(33):71-77.
16. Thair L, Kamachi Mudali U, Rajagopalan S, Asokamani R, Raj B. Surface characterization of passive film formed on nitrogen ion implanted Ti–6Al–4V and Ti–6Al–7Nb alloys using SIMS. Corros Sci. 2003;45(9):1951-1967.
17. Thair L, Kamachi Mudali U, Asokamani R, Raj B. Corrosion Properties of Surface Modified Ti-6Al-7Nb Alloy under Pulsed Plasma Nitriding and Nitrogen Ion Implantation Conditions. Surf Eng. 2004;20(1):11-16.
18. Du X-k, Wang T-m, Wang C, Chen B-l, Zhou L. Microstructure and Optical Characterization of Magnetron Sputtered NbN Thin Films. Chinese Journal of Aeronautics. 2007;20(2):140-144.
19. Bekermann D, Barreca D, Gasparotto A, Becker HW, Fischer RA, Devi A. Investigation of niobium nitride and oxy-nitride films grown by MOCVD. Surface and Coatings Technology. 2009;204(4):404-409.
20. Arslan E. Structural, mechanical and corrosion properties of NbN films deposited using dc and pulsed dc reactive magnetron sputtering. Surf Eng. 2010;26(8):615-619.
21. Kim SK, Cha BC, Yoo JS. Deposition of NbN thin films by DC magnetron sputtering process. Surface and Coatings Technology. 2004;177-178:434-440.
22. No YJ, Roohani-Esfahani S-i, Zreiqat H. Nanomaterials: The Next Step in Injectable Bone Cements. Nanomedicine. 2014;9(11):1745-1764.
23. Zoppi G, Beattie NS, Major JD, Miles RW, Forbes I. Electrical, morphological and structural properties of RF magnetron sputtered Mo thin films for application in thin film photovoltaic solar cells. Journal of Materials Science. 2011;46(14):4913-4921.
24. Khalaf MK, Hassan NK, Khudiar AI, Salman IK. Photoconductivities of Nanocrystalline Vanadium Pentoxide Thin Film Grown by Plasma RF Magnetron Sputtering at Different Conditions of Deposition. Physics of the Solid State. 2020;62(1):74-82.
25. Oladijo SS, Akinlabi ET, Jen TC, Mwema FM, Oladijo OP. Effect of power and deposition time on sputtered hydroxyapatite thin film coatings on stainless steel 304. Materials Today: Proceedings. 2022;62:4584-4588.
26. Khalaf MK, Mazhir SN, Mahdi MS, Taha SK, Bououdina M. Influence of RF sputtering power on surface properties and biocompatibility of 316L stainless steel alloy by deposition of TiO_2 thin films. Materials Research Express. 2018;6(3):035401.
27. Chen Q, McEwen GD, Zaveri N, Karpagavalli R, Zhou A. Corrosion resistance of Ti–6Al–4V with nanostructured TiO 2 coatings. Emerging Nanotechnologies in Dentistry: Elsevier; 2012. p. 165-179.
28. Muslim IdanHamil, Mohammed K. Khalaf, Mundher AL-Shakban, A Study Corrosion Properties by Magnetron Sputtered Nanocrystalline Al_2O_3 Thin Films, Egypt. J. Chem., 65, 11, 413-419 (2022).
29. Atapour M, Rajaei V, Trasatti S, Casaletto MP, Chiarello GL. Thin Niobium and Niobium Nitride PVD Coatings on AISI 304 Stainless Steel as Bipolar Plates for PEMFCs. Coatings. 2020;10(9):889.
30. Porokhov NV, Sirotina AP, Pershina EA, Shibalov MV, Diudbin GD, Mumlyakov AM, et al. Investigation of the superconducting properties of NbN films deposited by DC magnetron sputtering on a high-k dielectric HfO_2 buffer layer. Superconductor Science and Technology. 2021;34(11):115016.
31. Mukaromah UA, Andriyanti W, Sutanto H, Sahabudin NN. Layer deposition of titanium dioxide (TiO2) using DC-sputtering method with variation of deposition time: study of microstructure and coating hardness. Journal of Physics and Its Applications. 2021;4(1):14-19.
32. Tang J-F, Huang P-Y, Lin J-H, Liu T-W, Yang F-C, Chang C-L. Microstructure and Antimicrobial Properties of Zr-Cu-Ti Thin-Film Metallic Glass Deposited Using High-Power Impulse Magnetron Sputtering. Materials (Basel, Switzerland). 2022;15(7):2461.
33. Strzała A, Simka W, Marszałek M. Hydrothermal Synthesis of Hydroxyapatite on Titanium after Anodic Oxidation. Acta Physica Polonica A. 2012;121(2):561-564.
34. Okazaki Y, Rao S, Ito Y, Tateishi T. Corrosion resistance, mechanical properties, corrosion fatigue strength and cytocompatibility of new Ti alloys without Al and V. Biomaterials. 1998;19(13):1197-1215.
35. Gunawarman, Nuswantoro NF, Juliadmi D, Fajri H, Budiman A, Tjong DH, et al. Hydroxyapatite Coatings on Titanium Alloy TNTZ using Electrophoretic Deposition. IOP Conference Series: Materials Science and Engineering. 2019;602(1):012071.
36. Brancker AV. Quaternary Equilibria Data. Nature. 1950;166(4231):960-961.
37. Dinh TMT, Nguyen TT, Pham TN, Nguyen TP, Nguyen TTT, Hoang T, et al. Electrodeposition of HAp coatings on Ti6Al4V alloy and its electrochemical behavior in simulated body fluid solution. Advances in Natural Sciences: Nanoscience and Nanotechnology. 2016;7(2):025008.
38. Chitra P, Prashantha GS, Rao A. Long-term evaluation of metal ion release in orthodontic patients using fluoridated oral hygiene agents: An in vivo study. Journal of the World Federation of Orthodontists. 2019;8(3):107-111.
39. Kaaber K, Veien NK, Tjell JC. Low nickel diet in the treatment of patients with chronic nickel dermatitis. Br J Dermatol. 1978;98(2):197-201.
40. Leban MB, Kosec T, Finšgar M. Corrosion characterization and ion release in SLM-manufactured and wrought Ti6Al4V alloy in an oral environment. Corros Sci. 2022;209:110716.